Flux driven two-dimensional fluid turbulence simulation in the edge and scrape-off layer tokamak plasma

N. Bisai, A. Das, S. Deshpande, R. Jha, P. K. Kaw, A. Sen, and R. Singh

Institute for Plasma Research
Bhat, Gandhinagar-382 428, India

Abstract

A novel two-dimensional (2D) fluid model is proposed for investigating flux driven plasma turbulence in the tokamak edge and scrape-off layer (SOL). Unlike most previous simulations of this regions, our model treats the two regions in a consolidated manner with a smooth transition in between. Our unified 2D model is simpler and less computer intensive than three dimensional (3D) models, but captures most features of 3D edge and 2D SOL turbulence. It also illustrates the influence of tokamak edge turbulence on the SOL transport, something not captured by the earlier 2D SOL simulations. Existence of an equilibrium radial electric field in the edge and SOL regions is confirmed, this electric field is found to change sign in the edge-to-SOL transition regions. Turbulence in the edge is characterized by radially elongated streamers and zonal flows. The streamer structures occasionally break. We obtained phenomenological condition for the breaking of the streamers. Formations of density blobs and its dynamics in the edge and SOL regions have been studied. It is found that the blobs are created in the edge region where the radial electric field changes sign. All the blobs, which form in this regions are not ejected deep into the SOL. Only few of them are ejected. The ejection condition has been discussed. The effective diffusion co-efficient has been calculated from the simulation results and is found to be consistent with most tokamak experimental values. Statistical properties of the particle transport obtained from this simulation are compared with the earlier flux driven 2D SOL turbulence simulation results also with Aditya tokamak results.

1 Introduction

Flux driven turbulence in edge and in scrape-off layer (SOL) has been studied using numerical simulation codes in recent years. The edge turbulence related to resistive ballooning mode has been studied mainly using three dimensional (3D) code [1-3]. Simulations show radially extended convective cells (streamers) and zonal flows. The streamers are responsible for large intermittent transport. Zonal flows self-regulate the turbulence. The SOL simulations have been done using 2D codes [4-6] related to flux driven interchange instability and are capable to explain many experimentally observed facts like intermittent ballistic transport together with scale invariance in time of fluctuations and flux spectrum behavior similar to self-organized criticality. All the above edge and SOL simulations have been done separately in the edge and SOL regions. A major simplification in the 2D SOL simulation is the particle flux coming from the confined plasma into the SOL region is constant in time and in the poloidal direction. In reality, the driving flux originating from the edge turbulence has spatio-temporal variations. Therefore, a more accurate description of the SOL turbulence can be obtained by a combined edge and SOL turbulence simulations. In this work, we have joined the edge and the SOL turbulence using a novel 2D model related to resistive ballooning mode in the edge and interchange instability in the SOL. The model connects the two regions in a consolidated manner with smooth transition in between. Although our unified 2D model is simpler and less computer intensive than the 3D models, it captures most of the features of 3D edge and 2D SOL turbulence. The code shows an existence of radial electric field, $E \times B$ zonal flows and radially extend streamer structure. In this work, particular attention has been given to the streamer structure dynamics near edge-to-SOL regions, formation density blob, and the condition for its ejection deep into the SOL. An influence of edge turbulence on the SOL transport has been observed, which was not captured earlier by simple 2D SOL simulations. We have compared the statistical properties of particle flux with earlier 2D SOL simulation results and also with Aditya tokamak results.

2 Model equations and numerical simulation

Flux driven electron continuity and current balance equations have been used for the simulation. The detailed derivation of the model equations is given Ref [9]. The model equations are;

$$\frac{dn}{dt} + g(\frac{\partial n}{\partial y} - n\frac{\partial \phi}{\partial y}) - D_\perp \nabla_\perp^2 n = -\sigma_0 \sigma(x) n e^{\Lambda - \phi} + \chi_0 \chi(x)(\phi - \langle\phi\rangle_y - n + \langle n\rangle_y) + S_n \quad (1)$$

$$\frac{d\nabla_\perp^2 \phi}{dt} + \frac{g}{n}\frac{\partial n}{\partial y} - \nu \nabla_\perp^4 \phi = \sigma_0 \sigma(x)\left(1 - e^{\Lambda - \phi}\right) + \chi_0 \chi(x)(\phi - \langle\phi\rangle_y - n + \langle n\rangle_y) \quad (2)$$

where $d/dt = \partial/\partial t + \mathbf{v}_E.\nabla_\perp$, $\nabla_\perp = \hat{x}\partial/\partial x + \hat{y}\partial/\partial y$, and $\mathbf{v}_E = \mathbf{E} \times \mathbf{B}/B^2 = -\nabla_\perp \phi \times B/B^2$; $\mathbf{B}$ is toroidal magnetic field , $\mathbf{E}$ is electric field ($\mathbf{E} = -\nabla_\perp \phi$), ϕ is electrostatic potential, x and y denote radial and poloidal co-ordinates. Term $\langle f\rangle_y$ denotes poloidal average of f. Here, n and ϕ denote density and potential normalized by arbitrary density n_0 and T_0/e (e is electronic charge, T_0 is electron temperature) respectively. Time t is normalized by Ω_s^{-1}, where $\Omega_s (= eB/m_i)$ is ion cyclotron frequency, m_i is ion mass. Co-ordinates (x, y) are normalized by ion gyro-radius $\rho_s (= c_s/\Omega_s)$, $c_s = (T_0/m_i)^{1/2}$. The term g represents normalized gravity denoted by $g \equiv \rho_s/R$ and $D_\perp$, $\nu_\perp$ are diffusion coefficient and viscosity normalized by $\rho_s c_s$. The driving source is modeled by $S_n = S_0 \exp[(-x/\lambda_s)^2]$, where S_0 is maximum amplitude of the source normalized by $n_0\Omega_s$ and λ_s is e-folding source width. The region $x \leq 0$ ($x \geq 0$) with positive (negative) density gradient models high (low) field side of a tokamak. The floating potential is denoted by $\Lambda \equiv 0.5 \ln[4/\pi m_i/m_e]$, m_e is electron mass. The terms σ_0 and χ_0 denote normalized maximum sheath conductivity and normalized parallel plasma conductivity. These are denoted by $\sigma_0 \equiv \rho_s/L_c$ and $\chi_0 \equiv (\rho_s/qR)^2(m_i/m_e)(\Omega_s/\nu_e)$ where L_c is parallel connection length, R is major radius, q is safety factor and ν_e is collision frequency with the background plasma. The terms $\sigma(x)$ and $\chi(x)$ are models of sheath conductivity and parallel plasma conductivity respectively, $\sigma(x) = 0.5(2 + \tanh[(x - x_0)/\delta_0] - \tanh[(x + x_0)/\delta_0]$ and $\chi(x) = (1 - \sigma(x))exp(-|x|/l_\chi)$, where x_0, δ_0, and l_χ denote width of the edge and width of the edge-to-SOL transition region and e-folding length of the edge plasma conductivity profile.

The input parameters for the simulation corresponds to typical tokamak edge and SOL parameters [9]. We have carried out the simulation using the following parameters $D_\perp = \nu_\perp = 0.01$, $g = 8 \times 10^{-4}$, $S_0 = 5 \times 10^{-4}$, $\Lambda = 3.9$, $\lambda_s = 5.0$, $\sigma_0 = 2 \times 10^{-4}$, $\delta_0 = 3.0$, $l_\chi = 15.0$ and $x_0 = 25.0$. The value of χ_0 has been varied from 2.5×10^{-4} to 2×10^{-3}. Eqs. (1)-(2) are solved using pseudo-spectral code [6]. Periodic boundary condition has been used in the radial and poloidal directions.

3 Simulation results

Simulation shows a self-consistent generation of radial electric field E_x. Average of E_x over time and poloidal direction denoted by $\langle E_x\rangle_{y,t}$ and its shear $d\langle E_x\rangle_{y,t}/dx$ are shown in Fig. 1(a)-(b). It is to be noted that E_x changes sign near $x = 18$ and $x = 38$, and its shear is maximum near these positions. Fig. 1(a) shows the zonal flow along ion diamagnetic direction in the edge region. The maximum zonal flow obtained from the simulation is about 3.0 km/s for typical Aditya tokamak parameters. Simulations have been done with different values of χ_0. Results show $\langle E_x\rangle_{y,t}$ increases with the increase of χ_0 [6].

Radially elongated streamer structure of turbulent particle flux denoted by $\Gamma(x, y) = -n\partial\phi/\partial x$ has also been observed in our simulation. It is to be noted that similar structure has also been reported in earlier 3D edge turbulence simulations [1-3]. Here, we have studied its dynamics near edge-to-SOL transition regions. It is found that most streamers break or deform near outer edge regions, where the E_x changes sign and shear has its maximum value. Fig. 2(a) shows streamer structure breaking. Fig. 2(b) (taken after 400 normalized time of breaking) shows shear structure movement both in the radial and poloidal directions. The shear makes different parts of the streamer to move with different poloidal velocities. Therefore, different parts of the structure get a net displacement with respect to each other. If resultant displacement between major two parts during the eddy-turn-over time is greater than the poloidal width of the streamer, the streamer breaks into two. Mathematically, the condition of breaking is;

$$(\langle\partial E_x/\partial x\rangle/\langle E_y\rangle) \times \delta_x^2 \geq \delta_y \quad (3)$$

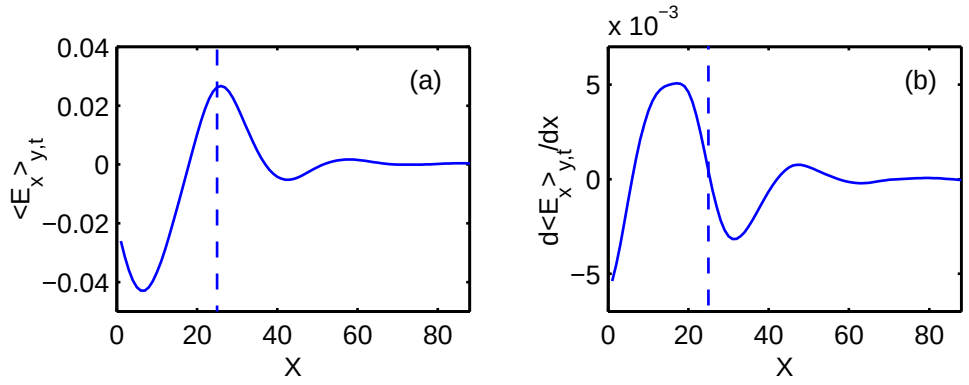

Figure 1: Poloidal and time average of E_x [Fig. 1(a)] and its shear [Fig. 1(b)]. Vertical line show edge-to-SOL transition.

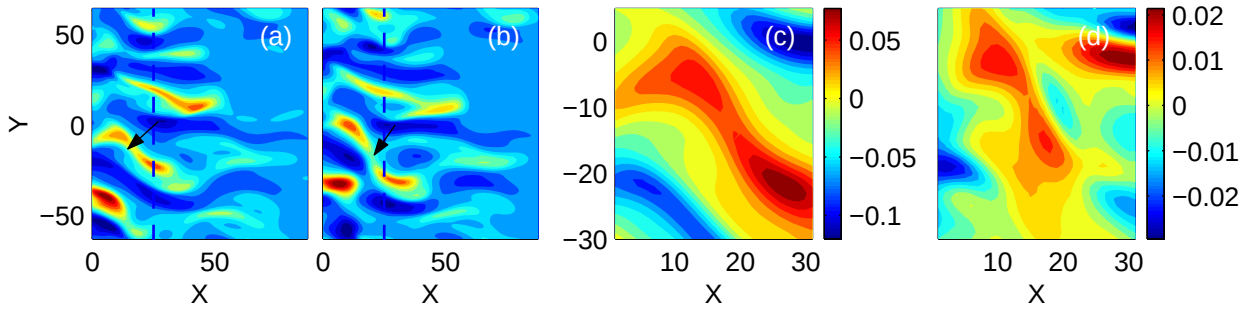

Figure 2: Flux streamer during its breaking [Fig. 2(a)] and after breaking [Fig. 2(b)]. Plots of E_x and $\partial E_x/\partial x$ at the position of breaking are shown in Figs. 2(c)-(d). The arrows indicate the position of the breaking.

where $\langle f \rangle$ indicates average of f over the radial length of the streamer, δ_x is radial distance between maximum and minimum values of E_x near $x = 18$, and δ_y is poloidal width of the streamer. Figs. 2(c)-(d) show E_y and $\partial E_x/\partial x$ at the breaking location. Figs. 2(a)-(d) indicate $\langle E_y \rangle \sim 0.04$, $\langle \partial E_x/\partial x \rangle \sim 0.01$, $\delta_x \sim 15$, $\delta_y \sim 15$, consequently the breaking condition is satisfied. The similar streamer breaking has also been observed near $x = 38$ position.

Simulation shows both high and low density events traveling outward and inward directions in the edge and SOL regions. We have measured radial propagation velocities V_x of density structure that have density greater than 1.5 times of average density ($\bar{n}$) for different values of χ_0. The probability distribution function (PDF) at (20,0) and (35,0) for $\chi_0 = 2 \times 10^{-3}$, 2.5×10^{-4} are shown in Fig. 3(a). In the edge, the PDFs show that the higher positive velocities are more probable for lower values of χ_0. This indicates that the velocity mainly depends on collisionality of the plasma rather than density scale length a. It is to noted that the density scale length for $\chi_0 = 2 \times 10^{-3}$, and 2.5×10^{-4} are about 10-18ρ_s and 15-25ρ_s respectively. Therefore, smaller structures are not moving faster velocities in compared to larger structures. The smaller structures are also more probable to move inward direction than the larger structures. In the SOL, most probable radial velocity for higher χ_0 is higher. These are about $0.04c_s$ and $0.06c_s$ for $\chi_0 = 2.5 \times 10^{-4}$ and 2×10^{-3} respectively. Simulation shows that the radial velocity depend on the scale length ($V_x \sim a^{-2}$) as turbulence is mainly controlled by sheath physics rather than collisionality of the plasma. It is to be noted that all blobs are moving mainly outward directions. Diffusion in the edge and SOL is believed to be by the motion of these structures. We have calculated effective diffusion coefficient $D_{eff} = -\langle \Gamma_\perp(x,t) \rangle_t / \langle \partial n(x,t)/\partial x \rangle_t$ from the simulation data. The D_{eff} in the edge highly depends on the χ_0 and in the SOL its effect is small but it is still higher for smaller value of χ_0. Fig. 3(b) shows plot of D_{eff} in the edge and SOL regions for $\chi_0 = 2 \times 10^{-3}$ (solid line), 5×10^{-4} (dashed-doted line), and 2.5×10^{-4} (dashed line).

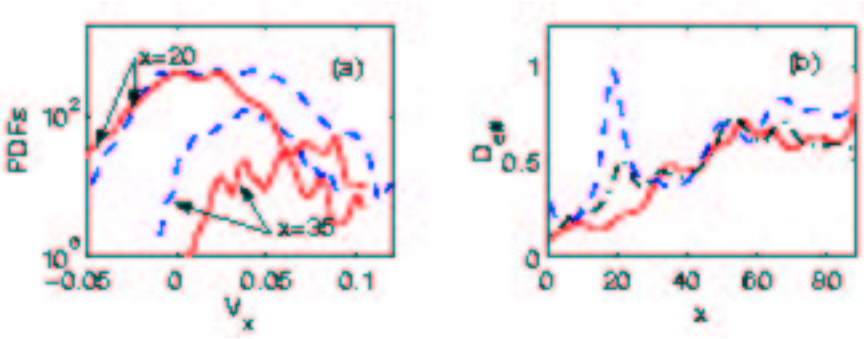

Figure 3: PDFs of radial velocities of density structure [Fig. 3(a)] and D_eff [Fig. 3(b)]. The solid and dashed lines in Fig. 3(a) indicate PDFs at (20,0) and at (35,0) for $\chi_0 = 2 \times 10^{-3}$, 2.5×10^{-4} respectively. The solid, dashed-dot and dashed lines in Fig. 3(b) indicate diffusion coefficients for $\chi_0 = 2 \times 10^{-3}$, 5×10^{-4}, and 2.5×10^{-4} respectively.

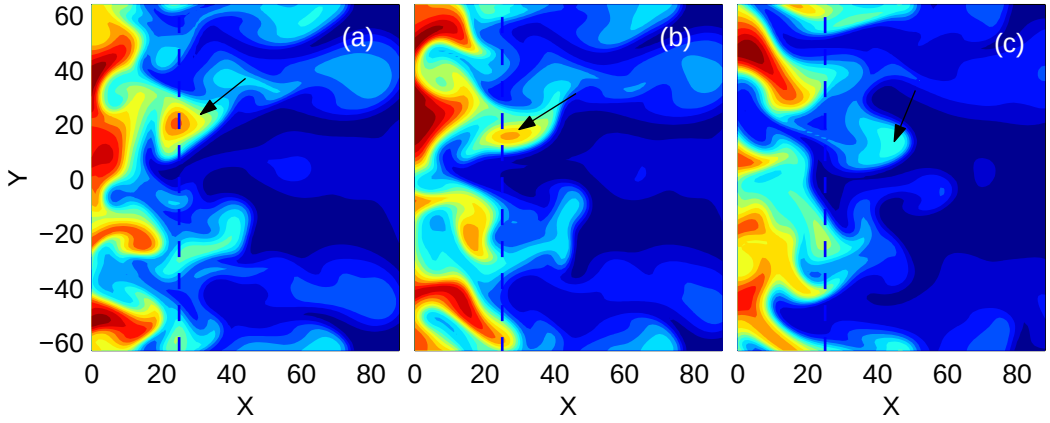

Figure 4: Formation of density blob Fig. 4(a) and its radial and poloidal motion Figs. 4(b)-(c). Note the motion of the blob indicated by arrow. Fig. 4(c) shows blob ejection into the SOL. Time interval between two successive figures is 200 normalized time.

Detachment of density structure from the main plasma has been observed. Radially elongated density streamer breaks in the edge mainly at the position, where the E_x changes sign and its shear is maximum. The detached structure form like a blob as shown in Fig. 4(a). The condition of density blob formation is same as given in Eq. (3). The detached blob moves in a complicated manner in the edge and in the SOL. The radial motion of the blob in the SOL is mainly due to ∇B polarization and associated $E \times B$ drift. Blob rotation is seen mainly in the edge-to-SOL transition region. It depends on both curvature induced potential [8] also on $\chi_0\chi(x)(\tilde{n} - \tilde{\phi})$ in Eqs. (1)-(2), where $\tilde{n} = n - \langle n \rangle_y$ and $\tilde{\phi} = \phi - \langle \phi \rangle_y$. Dependence of the blob rotation on the $\chi_0\chi(x)$ and its associated stabilization due to charge mitigation [8] effect will be presented elsewhere. Radial and poloidal motion of a blob are shown in Fig. 4(a)-(c). All the blobs which form near outer edge region are not ejected deep into the SOL. Many blobs form and die out without much movement. We have studied the condition for the blob ejection. It is found that bigger blobs which have sufficiently long life time (τ_{life}) eject deep into the SOL whereas smaller blobs die out before ejection. The blob seems to eject into the SOL from the transition region if $E_y \times \tau_{life} \simeq 15\rho_s$ is satisfied.

The turbulent particle flux in the edge (15,0) and in the SOL (40,0) has been measured [Fig. 5(a)-(b)]. An influence of edge turbulence on the SOL turbulence has been found. The edge instabilities induce plasma injection into the SOL region, which modify the SOL equilibrium profile and drives an instability in the SOL region. When compared to the experiments, we find that skewness (1.6 in the edge and 3.6 in the SOL) and kurtosis (8.0 in the edge and 16.0 in the SOL) are close to the experimental values

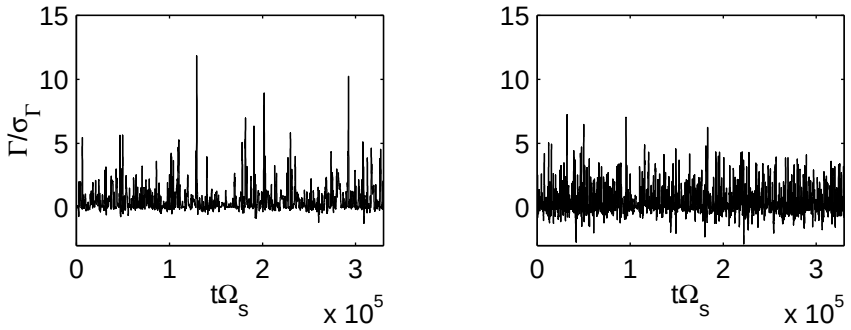

Figure 5: Flux time series Γ (normalized by standard deviation of Γ) in the edge (right hand side figure) and in the SOL (left hand side figure).

(skewness=3.8 and kurtosis=38.0). Flux driven 2D SOL turbulence result shows that the skewness and kurtosis are 1.7 and 7.7 [6]. This result deviates more from the experimental results than the joint 2D edge and SOL simulation results. This clearly demonstrates the influence of edge turbulence on the SOL.

In this work, we have presented a novel 2D edge and SOL turbulence simulation using a single code. The model is very simple but it captures many features of 3D edge and 2D SOL turbulence results. It also illustrates the influence of edge turbulence on the SOL. Dynamics of streamer structures in the edge and SOL has been simulated. The structures occasionally break. We have derived a condition of the breaking. Change of sign of radial electric field and its shear are responsible for density blob formation. Normally small blobs form in the edge region and die out without much radial movement. Only bigger blobs are capable to eject deep into the SOL. A condition of blob ejection into the SOL has been derived. Statistical properties of particle flux obtained from this simulation are close to the experimental results.

References

[1] Benkadda, S., et.al., Nucl. Fusion **41** 995 (2001)

[2] Beyer, P., et. al., Phys. Rev. Lett. **85**, 4892 (2000)

[3] Benkadda, S., et.al., Phys. Scripta **T84**, 14 (2000)

[4] Sarazin, Y., Phys. Plasmas **5**, 4214 (1998)

[5] Garcia, O. E., et.al., Phys. Rev. Lett. **92**, 165003 (2004)

[6] Bisai, N., Phys. Plasmas **11**, 4018 (2004)

[7] Krasheninnikov, S. I., Phys. Lett. **A 283**, 368 (2001)

[8] Myra, J. R., et.al., Phys. Plasmas **11**, 4267 (2004)

[9] Bisai, N., et.al., submitted to Phys. Plasmas